

## VIBRATION STUDIES OF HOIST-CUM-ELEVATOR SHAFTS IN FILL FOR BEAS DAM AT PONG

A. S. Arya\*, Y. P. Gupta\*\* and N. Gosain†

### INTRODUCTION

The problem of earthquake resistant design of Hoist-cum-Elevator Shafts in fill for Beas Dam at Pong was referred to the School of Research and Training in Earthquake Engineering, University of Roorkee, by the General Manager, Beas Project, Talwara Township, for analytical and experimental seismic investigations. The description of structure, geology, location and other details are given in a Memorandum of Beas Designs on the subject. The structure is briefly described below :

### THE STRUCTURE

After the diversion stage is over, two diversion tunnels, namely  $T_1$  and  $T_2$ , will be used as outlet tunnels and will serve to cater for the discharge requirements of the irrigation

channels. Conduits of size  $7' \times 10'6''$  will be installed in the plug of each tunnel. To regulate flow through these conduits a set of emergency and regulating gates are to be installed. The operation of these gates shall be accomplished through two vertical shafts, called the 'Hoist-cum-Elevator Shafts' connecting the control section of the tunnels to the top of the dam at El. 1430 on upstream of the dam axis. The shafts are partly in rock and partly in fill which will be carefully compacted as the construction of the shafts proceeds. The portion of the shafts in fill is to be studied with respect to earthquake effects. The heights of the two shafts  $T_1$  and  $T_2$  in fill are 69 ft. and 90 ft. respectively.

The position of the shafts in plan is shown in Fig. 1 and the sectional view shown in Fig. 2. There is hard rock on one side of the shaft and on the other side a retaining wall. The proposed section of side shaft is circular with 12 ft. finished internal diameter and 2 ft or 1.5 ft uniform thickness. A shaft house of size  $14'6'' \times 15' \times 28'9''$  high, shall be constructed eccen-

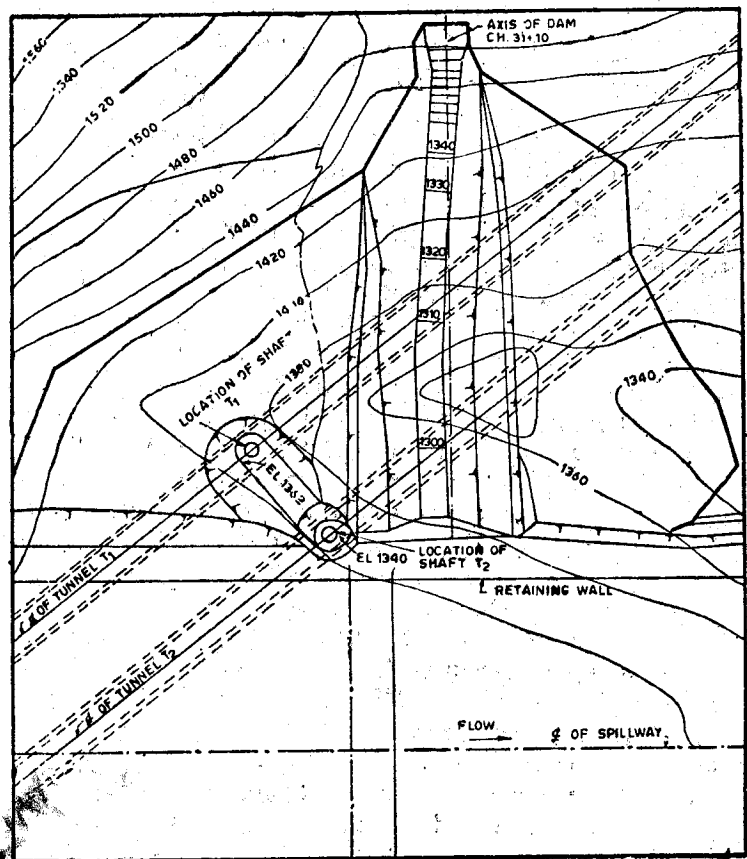


Fig. 1. Position of Shafts in Plan

\* Member, Professor and Assistant Director, School of Research and Training in Earthquake Engineering University of Roorkee, Roorkee, U. P., India.

\*\* Member, Lecturer, School of Research and Training in Earthquake Engineering, University of Roorkee, Roorkee, U. P., India.

† Member, Lecturer, School of Research and Training in Earthquake Engineering, University of Roorkee, Roorkee, U. P., India.

trically at the top of each shaft at El. 1430 for the installation of control machinery etc.

**OBJECTS OF INVESTIGATION**

The objects of the investigation are to study analytically and experimentally the influence of soil fill on the stiffness, damping and natural period of the structure to work out the forces and moments caused in the structure due to the earthquake selected for design for the site, and to design the section of the shafts.

**FORCES EXPECTED DURING AN EARTHQUAKE AND CONSEQUENT STRUCTURAL BEHAVIOUR**

Earthquake shocks cause random movement of ground in any direction producing vibrations in structures. The vibrations may be resolved in any three perpendicular directions. Vibrations in vertical direction are normally small and will only alter the weight of shaft. No appreciable differential vertical movement is expected to occur between the shaft and soil because of the rigidity of the shaft and stiffness of the compacted dense soil. Since the shaft house is partly cantilivered from the top of the shaft, the vertical component of earthquake will induce additional stresses in its walls. But these additional stresses will not be critical in the design since their effect will be absorbed in the permissible increase in working stresses. It is only the lateral movement which gives rise to differential movements inducing thereby additional moments and shears. Hence predominant direction of vibrations is horizontal. Now the shafts are completely surrounded by compact soil from all sides and the soil itself is confined because of the existence of hill, retaining wall and the body of the dam. Moreover, the depth of fill is not large, being only 90 ft maximum at a point, large relative movements within the soil mass are not expected to occur. Therefore, the shaft will be stressed because of their motion relative to the soil. Naturally the soil will tend to resist the motion of the shaft. Thus during an earthquake, the shafts will vibrate as a cantilever beam supported elastically by the soil all round. Since the soil is capable of applying the restraining effect to the motion of the shaft in either direction from its equilibrium position, therefore the shafts may be analysed assuming them as a beam on elastic foundation as shown in figure 3.

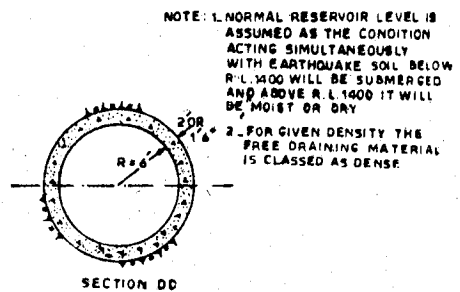
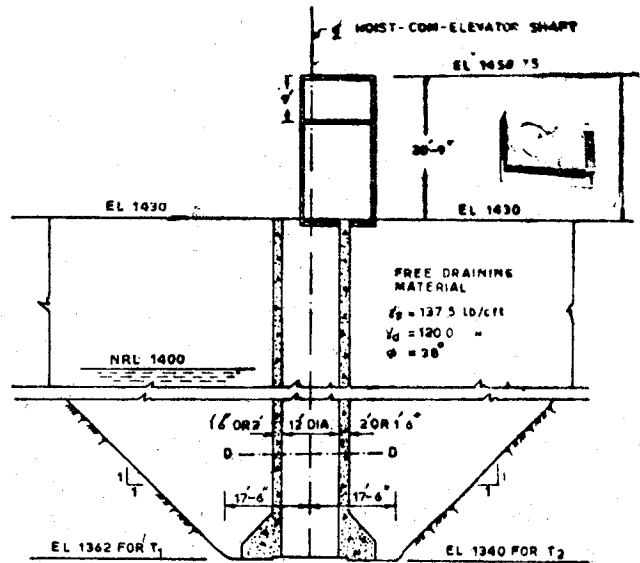


Fig. 2. Sectional View of Shafts in Fill

will induce additional stresses in its walls. But these additional stresses will not be critical in the design since their effect will be absorbed in the permissible increase in working stresses. It is only the lateral movement which gives rise to differential movements inducing thereby additional moments and shears. Hence predominant direction of vibrations is horizontal. Now the shafts are completely surrounded by compact soil from all sides and the soil itself is confined because of the existence of hill, retaining wall and the body of the dam. Moreover, the depth of fill is not

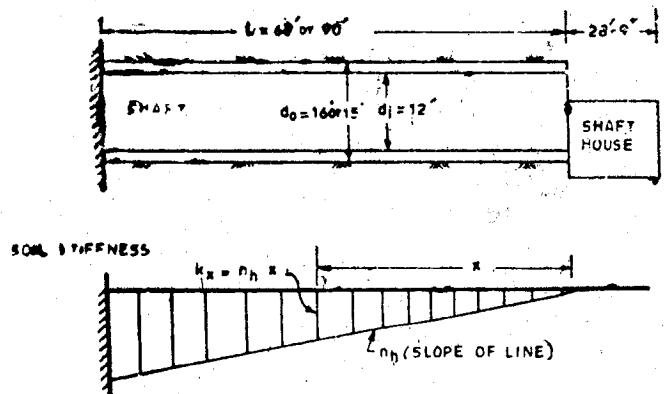


Fig. 3. Cantilever Shaft Supported on Elastic Foundation

## SOIL STIFFNESS

It is known that the modulus of subgrade reaction or the stiffness of cohesionless granular soils varies linearly with depth, being zero at the ground surface and maximum at the bottom<sup>(2,6)</sup>. This is normally defined in terms of the slope of stiffness variation line 'n<sub>h</sub>' as shown in Figure 3. Thus at any depth x below the ground surface, the modulus of subgrade reaction is given by

$$k_x = n_h x \quad (1)$$

It is also shown<sup>(2,6)</sup> that soil stiffness is independent of the width or diameter of the shaft. Therefore k<sub>x</sub> is the reaction offered by the soil per unit height of the shaft per unit of deflection. Taking k<sub>x</sub> as lb/in<sup>2</sup>, the units of n<sub>h</sub> become lb/in<sup>3</sup>. For cohesionless sands with various densities the values of the coefficient n<sub>h</sub> as recommended by Terzaghi (1955) are given in Table 1.

In the case under study, the densities of the back fill are as follows :

Saturated unit weight  $\gamma_s = 137.5$  lb/cft

Moist unit weight  $\gamma_d = 120.0$  lb/cft

Angle of internal friction  $\phi = 38^\circ$

Thus the soil belongs to the *dense* category and the following values of n<sub>h</sub> are adopted (see Note 1, Fig. 2)

For dry soil above RL 1400 75 lb/in<sup>3</sup>

For submerged soil below RL 1400 45 lb/in<sup>3</sup>

 Table 1. Values of n<sub>h</sub>

Sand	n <sub>h</sub> in lb/in <sup>3</sup>	
	Dry or Moist	Submerged
Loose ( $\gamma_d = 80$ lb/cft)	9.4	5.3
Medium ( $\gamma_d = 100$ lb/cft)	28.0	19.0
Dense ( $\gamma_d = 120$ lb/cft)	75.3	45.0
Very loose under repeated loading		1.5

## VIRTUAL MASS OF SOIL

It is well known that when a body vibrates under water, its frequency is reduced as compared with that in air. Since the stiffness of the body does not change, the decrease in frequency is attributed to a virtual mass of water which is supposed to be vibrating along with the body. When a body vibrates in soil, the soil offers resistance to the vibration of the body and contributes a large amount of stiffness to it. Whether it imparts a virtual mass as well or not, is not known. Experiments as described on page 17 were carried out on models of shaft T<sub>1</sub> in an attempt to separate the stiffness and virtual mass effects of the soil. But the separation of the two has not been possible. In the absence of any positive evidence but on the basis of the cylinder analogy<sup>(3,4)</sup> applied to above bodies vibrating in water, the virtual mass of soil is *assumed* here as the mass of a soil cylinder of the same diameter as the external diameter of the shaft, the unit weight of the soil in the cylinder being taken as below :

Above R. L. 1400  $120 \times \frac{1 - \sin 38^\circ}{1 + \sin 38^\circ} = 28.6$  lb/cft.

Below B. L. 1400  $62.5 + 75 \times \frac{1 - \sin 38^\circ}{1 + \sin 38^\circ} = 80.3$  lb/cft.

### MATHEMATICAL MODEL OF SHAFT

The idealised mathematical model of shaft is shown in Fig. 4. The shaft has been discretised at  $n+1$  equally spaced points giving  $n$  segments. It is assumed that the weight and soil reaction of a segment of shaft is lumped at each point. The masses are connected with each other by elastic weightless bars. The weight of the shaft-house has been lumped at three points. The end mass is at the free end of the cantilever. The bottom end of the shaft is taken as fixed. At each point there are four quantities to be determined namely shear  $V$ , moment  $M$ , slope  $\theta$  and deflection  $y$ . At the fixed end slope and deflection are known (both are zero) and shear and moment are to be found out. Let these be  $V_1$  and  $M_1$ . Similarly at the free end, moment  $M_F$  and shear  $V_F$  are known to be zero and slope and deflection are unknown. The unknown quantities are determined starting from the fixed end by writing transfer equations for each point in terms of the two unknowns  $V_1, M_1$ . The recurrence relations for two consecutive points and segments are obtained for two cases of seismic coefficient loading and vibration analysis as follows :

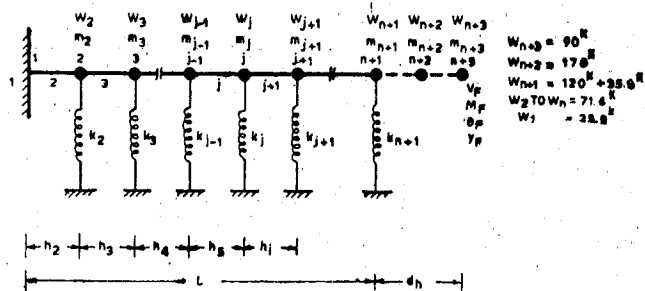


Fig. 4. Mathematical Model of Shaft when Supported on Elastic Foundation

#### (a) Seismic Coefficient Analysis

If the horizontal seismic coefficient is  $\alpha_h$ , the seismic load applied at any point  $j$  will be  $\alpha_h W_j$ . Then considering the bending and shearing deflections both, we have

$$V_j = V_{j-1} + (\alpha_h W_{j-1} - k_{j-1} y_{j-1}) \quad (2)$$

$$M_j = M_{j-1} + V_j h_j \quad (3)$$

$$\theta_j = \theta_{j-1} + \frac{h_j}{2E} \left( \frac{M_{j-1}}{I_{j-1}} + \frac{M_j}{I_j} \right) \quad (4)$$

$$y_j = y_{j-1} + \theta_{j-1} h_{j-1} + \frac{h_j^2}{3E} \left( \frac{M_{j-1}}{I_{j-1}} + \frac{M_j}{2I_j} \right) - \frac{C_s V_j h_j}{G A_j} \quad (5)$$

In expression (5),  $C_s$  is the shape factor for shear deformations.

#### (b) Vibration Analysis

In free-vibration analysis for determining a natural frequency  $p$  and the corresponding mode shape, we have the inertia forces  $p^2 m_j y_j$  acting at any point  $j$  instead of  $\alpha_h W_j$  in the above case. Besides, the rotary inertia will also act due to the rotation of the segment given by  $-p^2 \rho h_{j-1} I_{j-1} \theta_{j-1}$  where  $\rho$  is the mass of the shaft per unit length. The mass  $m_j = W_j/g$  where  $g$  is the acceleration due to gravity. Thus instead of equations (2) and (3) we get

$$V_j = V_{j-1} + (p^2 m_{j-1} - k_{j-1}) y_{j-1} \quad (6)$$

$$M_j = M_{j-1} + V_j h_j - p^2 \rho h_{j-1} I_{j-1} \theta_{j-1} \quad (7)$$

Equations (4) and (5) remain unchanged.

Equations (2) to (7) are applicable for all points but for  $n+2$  and  $n+3$ , the soil stiffness  $k_{n+2}$  and  $k_{n+3}$  are zero. Applying them successively to all the points and segments of the shafts starting with  $j=2$  the forces and displacements at all intermediate points  $j=2$  to  $j=n+2$  as well as the other end of the beam,  $j=n+3$  can be written. All these will involve  $V_1$  and  $M_1$  only as unknown since  $\theta_1$  and  $y_1$  are zero. Finally it is known that the shear  $V_F$  and moment  $M_F$  at the free end  $j=n+3$  are zero. This will give the equations for determining  $V_1$  and  $M_1$  in the seismic coefficient analysis and two homogeneous equations involving  $p^2$  in case of free vibration analysis which can be solved to calculate  $p$ . Using  $V_1$  and  $M_1$  the force and displacements in the shaft can be calculated at all points again using the transfer equations, and using  $p$  the mode shape can be similarly derived. The forces and moments in the later case may then be determined by the modal method using the relevant response spectra<sup>(9)</sup> for displacement giving the displacement  $S_d$  for various natural time periods and damping.

### CONDITION OF SHAFTS CONSIDERED IN ANALYSIS

The shafts have been divided in elements of small length, 17 elements of 4 ft each in case of  $T_1$  and 20 elements of 4.5 ft for  $T_2$ . The values of  $n_h$ , namely, 75 lb/in<sup>3</sup> for dry soil above R.L. 1400 and 45 lb/in<sup>3</sup> for submerged soil below this level have been used.

Other conditions considered are : (i) Shaft  $T_1$  is in air, that is, no soil is around, with shaft house at top, thickness of shaft 2 ft. ; (ii) Shafts  $T_1$  and  $T_2$  have soil stiffnesses as given above, and no virtual mass of soil is considered; Thickness is 2' and 1'6"; and (iii) Shafts  $T_1$  and  $T_2$  have soil stiffnesses as given above and a virtual soil mass is considered as explained earlier. Thickness of shaft is 2' and 1'6" as considered earlier.

In each of the above cases, moments and shears are worked out under the conditions of loadings : (i) Design seismic coefficient of 0.15 applied statically as adopted for designing the structures at the site of the Beas dam ; (ii) Modal analysis using response spectra of El Centro earthquake of 1940 (North-South Component) toned down to 0.17 g peak ground acceleration as recommended for Beas Dam site for elastic design of structures ; and (iii) Modal analysis using El. Cento earthquake of 1940 (N-S component, see Fig. 5) without reduction considered to be maximum probable for Beas Dam site.

Besides the moments caused by the seismic loadings, bending moments and shears are caused in the shaft due to eccentric placing of the shaft-house on top. These shears and moments have also been worked out and superimposed on the seismic shears and moments for finding the maximum values for design.

### ANALYTICAL RESULTS

#### (a) Free Vibration Analysis

Mathematical model as given in figure 4 was used in the dynamic analysis. For the various cases the

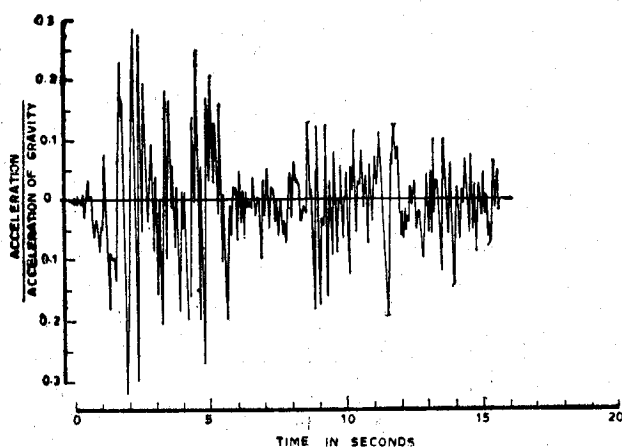


Fig. 5. Accelerogram For El Centro California Earthquake of May 18, 1940, Component N-S (Shown for 15 sec. only)

period of vibration and mode shape have been computed. Table 2 shows the fundamental periods of various cases, and corresponding spectral displacement values for El Centro 1940, N-S component are shown in Fig. 6 for various damping coefficients. A damping coefficient of 10% critical is adopted in the present case of  $S_d$  values given in Table 2 as explained later under experimental study. This value is on the conservative side for any appreciable relative movement of the shafts with respect to the soil.

(b) *Maximum Moments*

The maximum moments caused in the shafts  $T_1$  and  $T_2$  for thicknesses of 2 ft. and 1.5 ft. under the action of various loading conditions and various states of soil are presented in Table 3. The sections of the shaft where the maximum moments occur are also indicated, the distances being measured from the ground level, that is, below R. L. 1430.00. While finding combined maximum moments, the appropriate moments at the various sections of the shafts are to be added together (For example, see Table 4).

(c) *Observations on the Results in Tables 2 and 3*

The following observations can be made on the results presented in Tables 2 and 3:

(i) Whereas the fundamental time periods of the shafts  $T_1$  and  $T_2$  in air, without the soil around, are 0.4395 and 0.654 second respectively having a ratio 1 : 1.49, the time periods, when in soil, are about equal. This happens because the characteristic length of the shaft ' $L_c$ ' works out to be less than that of the shorter shaft. Therefore, their effective lengths which are subjected to flexure become nearly equal as shown below :

The characteristic length  $L_c$  is given by <sup>(5)</sup>

$$L_c = 5 \sqrt{\frac{EI}{n_h}} \quad (8)$$

where  $EI$  is the flexural rigidity of the shaft and  $n_h$  is the soil stiffness as defined on page 11. In the present case  $n_h = 75 \text{ lb/in}^3$ ,  $EI = 10450 \times 10^{10} \text{ lb-in}^2$  for 2 ft. thick shafts and  $6850 \times 10^{10} \text{ lb-in}^2$  for 1.5 ft. thickness. Therefore,  $L_c$  works out as 22.5' and 20.4' for 2 ft. and 1.5 ft. thickness of shaft respectively. These are less than the lengths of both the shafts  $T_1$  and  $T_2$ . Therefore, the critical length  $L_c$  is the same for both the shafts for any given thickness making their time periods about equal.

(ii) The shafts are in the low period range of the earthquake spectra indicating that they are stiff structures which would develop high dynamic forces due to earthquake but undergo small displacements.

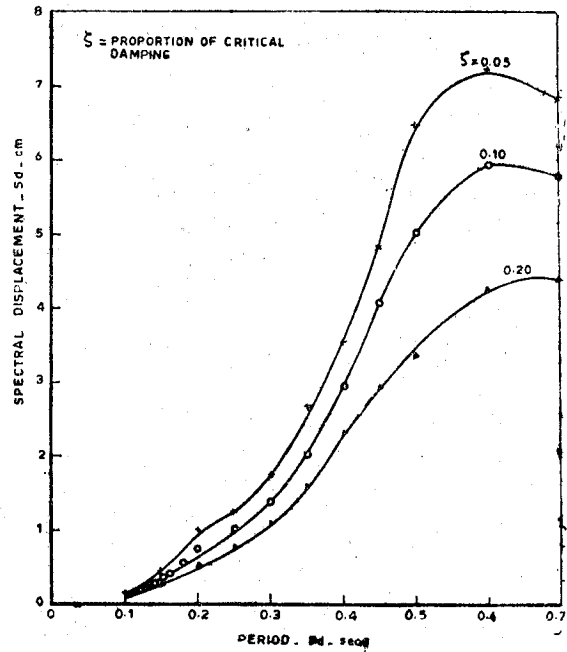


Fig. 6. Displacement Spectra of El Centro Earthquake, May 18, 1940, N-S Component

TABLE 2  
Time Periods and Spectral Displacement

(a) Thickness of shaft — 2 ft.

Condition of soil around shaft	Shaft T <sub>1</sub> (Ht. 68 ft)			Shaft T <sub>2</sub> (Ht. 90 ft)		
	Time period	S <sub>d</sub> for El Centro 1940		Time period	S <sub>d</sub> for El Centro 1940	
		peak Accn. 0.17g	Peak Accn. 0.33g		peak Accn. 0.17g	Peak Accn. 0.33g
	(second)	(cm)	(cm)	(second)	(cm)	(cm)
1. Shaft in air (no soil around)	0.4395	1.946	3.775	0.6540	3.030	5.875
2. Shaft in soil (no virtual mass)	0.2610	0.541	1.050	0.2639	0.552	1.070
3. Shaft in soil (cylindrical virtual mass).	0.2827	0.628	1.220	0.2870	0.644	1.250

(b) Thickness of shaft—1.5 ft. Shaft T<sub>2</sub> (Ht 90 ft)

Condition of Soil around Shaft	Time period	S <sub>d</sub> for El Centro 1940	
		Peak Accn. 0.17g	Peak Accn. 0.33g
	(Second)	(cm)	(cm)
1. Shaft in soil (no virtual mass)	0.2857	0.633	1.23
2. Shaft in soil (cylindrical virtual mass).	0.3054	0.722	1.40

Note :—Since the shafts are low period (high frequency) structures, the contribution of the higher modes than the fundamental is insignificant and therefore is not considered.

(iii) The periods are within the usual range of the ground periods recorded in strong ground motions. Therefore, quasi-resonance is likely to occur leading to appreciable amplification of the motion and high dynamic forces as indicated in (ii) above. But due to the random nature of the ground motion, full resonance build-up as in the case of steady state vibrations is not feasible. The high damping offered by the soil around the shaft is a further check on the high peaks in the response of the shaft.

(iv) The maximum moments, that would have occurred in the shafts, if they were standing in air, are very considerably reduced due to the presence of soil around the shafts. The reduction is about 70%. The section of maximum moment is shifted from the base of the shaft to a section within about the top 40% height of the shafts.

(v) Out of the two soil conditions, not taking virtual mass into account and with doing so, the latter situation gives higher moments in a shaft. It will, therefore, be critical for design.

Table 3  
Comparison of Maximum Moments

Condition of Soil	Max. Moments in kip-ft for loading condition and thickness						
	Eccentric load of Shaft House		Seismic Coeff 0.15		El Centro 1940 Peak acc. 0.17 g		El Centro 1940 Peak acc. 0.33g
	2 ft	1.5 ft	2 ft	1.5 ft	2 ft	1.5 ft	2 ft   2.5 ft
<b>A. Shaft T<sub>1</sub> (Ht. 68)</b>							
1. Shaft in air (no soil around)	2660 uniform	2660 uniform	9250 at base	—	27000 at base	—	52375 at base
2. Shaft in soil (no virtual mass)	2660 at top	2660 at top	1788 at 24'	1644 at 24'	6140 at 28'	—	11903 at 28'
3. Shaft in soil (cylindrical virtual mass)	2660 at top	2660 at top	1837 at 24'	1686 at 20'	8090 at 32'	—	15712 at 32'
<b>B. Shaft T<sub>2</sub> (Ht. 90)</b>							
1. Shaft in air (no soil around)	2660 at top	2660 uniform	—	—	28560 at base	—	55403 at base
2. Shaft in soil (no virtual mass)	2660 at top	2660 at top	1767 at 22.5'	1649 at 22.5'	6040 at base	5060 at 20.5'	11716 at 27' at 23.5'
3. Shaft in soil (cylindrical virtual mass)	2669 at top	2669 at top	1809 at 22.5'	12699 at 22.5'	7940 at 31.5'	6550 at 27'	15409 at 27' 12699' at 27'

The distances mentioned for the Section carrying maximum moment are measured below ground level 1430.0'



(vi) The maximum moments in the two shafts  $T_1$  and  $T_2$  are not appreciably different, the moments in shaft  $T_1$  being slightly higher than those in shaft  $T_2$ . Therefore, the same design values may be adopted for the two.

(vii) The maximum moments in the shaft obtained by dynamic analysis for El Centro *toned-down* earthquake (with peak ground acceleration 0.17g for the condition of soil with virtual mass are about 4.4 times as large as the maximum moments produced by static seismic coefficients of 0.15g applied uniformly to the shaft. Therefore, the design of the shafts on the basis of uniform seismic coefficient of 0.15g will be grossly inadequate and must be worked out for the forces determined dynamically.

(viii) The dynamic maximum moments for 1.5 ft. thickness are about 83% of those for 2.0 ft. thickness.

### EXPERIMENTAL STUDY

The object of this study was to observe the behaviour of the shaft under vibrating conditions. A geometrically similar model having a scale ratio 1/24 to the shaft  $T_2$  was used. The scale ratio of 1/24 was chosen for making the model to suit the shake table facilities and ready availability of a commercially manufactured concrete pipe of 6 in. diameter and 1 in. thickness. The length of the model required for 90 ft. long shaft on this scale was 3'9". The shake table container was deep enough to contain this depth.

Due to certain practical difficulties of having a scaled down shaft house in the model, it was considered easier to simulate its weight and overturning moment by protruding the pipe beyond the 3'9" mark of sand fill and mounting extra weights on top. The extra length used was 10 in.

For a geometrically similar model the similitude requirement is

$$\frac{w_m}{w_p} = \frac{l_p}{l_m} \cdot \frac{E_m}{E_p}$$

where  $w$  is the density of material,  $E$  the Young's Modulus of Elasticity,  $l$  the linear dimension and suffixes  $m$  and  $p$  refer to model and prototype respectively. This requires that the model material should have a high density and low elastic modulus. But for the model under consideration,  $w_m = w_p$  and  $E_m = E_p$  and  $l_p/l_m = 24$ . Therefore, this similitude requirement was violated in this model. Unfortunately this happens in most such experimental cases. Because of the difficulties experienced in satisfying all the similitude requirements it was not possible to have a model from which results for the prototype could be interpreted directly. Therefore, the model dimensions were used as such to determine its frequency.

The model was sited in the middle of the shake table container of size 6' 4" × 4'2" × 4'. The prototype has a conical frustum shaped rock excavation around it from El. 1340 upwards. A similar formation was reproduced on the table by means of a rich mix of plaster of paris and sand. The sand in the container was gradually filled upto elevation 1430 being compacted by tamping by wooden flat boards at their end.

The model was subjected to free vibration test by means of pulling it at top horizontally and letting it go suddenly. Accelerometers were mounted at the top and 8 in. and 16 in. below the top corresponding to El. 1434 and El. 1418 respectively. Free vibration records were taken on oscillographs. The shaft was tested without any super-

imposed load and with superimposed loads of 20, 30, 40 and 50 kg attached on its top. Records were taken for the shaft vibrating in the dry sand fill upto El. 1430. The observations were made in the following order of superimposed loads 00, 20, 30, 40 and 50 kg.

### Observations

The variation of frequency with superimposed load is shown in figure 7. It is seen that the reduction in the experimental frequency when top weight is increased is rather gradual and the drop is only 27 percent when the top weight becomes 50 kg. In the same figure theoretical frequencies calculated for two values of soil stiffness coefficients are also plotted which show that the theoretical frequency is more sensitive to the top weight than indicated by experimental curve. When virtual mass for dry soil according to cylinder analogy (see page 11) is considered, the frequency of vibration decreases and goes farther away from the experimental frequency.

The damping was observed as 6% of critical when the shaft was vibrating in air and 11% of critical when vibrating in sand fill.

### Discussion of Results

(a) *Soil Stiffness and Virtual Mass*: The observations show that the experimental frequency was higher than the theoretical frequency based on the  $n_h$  value of 75 lb/in<sup>3</sup> recommended by Terzaghi for dense sands. It is stated by Terzaghi that the recommended value is somewhat conservative and actual value may be higher. The use of virtual mass has the influence of reducing the theoretical frequency, further increasing the gap between theoretical and experimental frequencies. This indicates that no virtual mass of soil may actually be acting. However from the safety point of view of the structure it will be necessary to consider what would happen if (i) the soil stiffness becomes higher (ii) virtual mass acts.

From Fig. 7, it is seen that when the soil stiffness is increased from 75 lb/in<sup>3</sup> to 160 lb/in<sup>3</sup>, the frequency increases by 14% only. Thus the frequency is rather insensitive to increase in stiffness. Moreover, the range of frequency of the prototype shafts lie in the region of maximum acceleration response. Therefore, slight change of frequency will be immaterial in the response.

The virtual mass of soil has two influences: to decrease the frequency and to add to the vibrating mass which would increase the forces acting on the shaft. The first effect would compensate the effect of stiffness to some extent. The increase of force will of course be material in design. In view of the inconclusive results of the tests and to be on the safe side, calculations have also been made by using soil mass on the basis of cylinder analogy as discussed earlier.

(b) *Damping*: The damping increased from 6% in air to 11% of critical when vibrating in soil. This damping is expected to further increase if the deflections of the shaft increase. Therefore, a damping coefficient of 10% of critical was conservatively used in the calculation of forces.

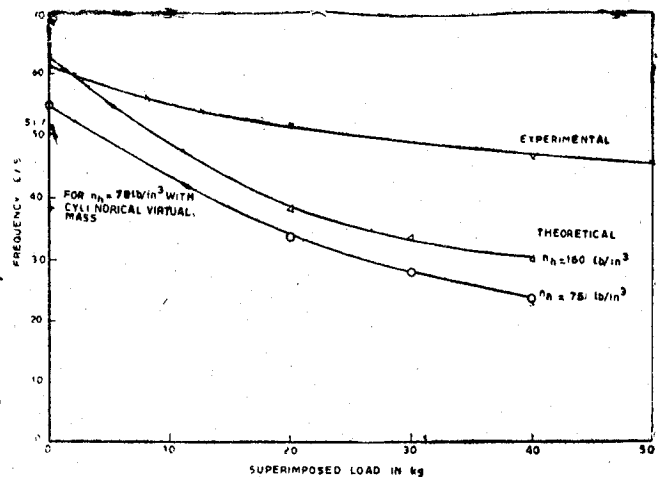


Fig. 7. Variation of Frequency with Superimposed Load on Top of Shaft Model.

### DESIGN CRITERIA

Based on the analytical and experimental results, the following criteria have been adopted for designing the shaft :

- (a) To use cylindrical virtual mass of soil for computing seismic moments and shears.
- (b) To use seismic moments as calculated for El Centro toned-down earthquake with peak ground acceleration 0.17 g for elastic design allowing the tensile stress in steel to just reach the yield stress but without allowing any plastic deformations.
- (c) To permit plastic yielding of the steel for the El Centro earthquake with peak ground acceleration of 0.33g. the ductility ratio,  $\mu$ , that is the ratio of maximum deformation to the yield point deformation however not being allowed to exceed 4.
- (d) To design the two shafts  $T_1$  and  $T_2$  to have the same thickness and reinforcement which may be kept uniform throughout the height of the shafts. This uniformity is adopted in view of the possibility of occurrence of an earthquake during construction and the time lag which may occur between the construction of the shafts and the placing of the back fill.
- (e) To impose the restriction that at no stage of construction, the back fill should be allowed to lag behind the shafts by more than 25 ft. This will keep the maximum moments in the shaft within the maximum design moments at all stages of construction in the event of the occurrence of an earthquake during construction.

### DESIGN OF SHAFTS

On the basis of the criteria recommended above, the design values of moments and shears in the top length of about 30 ft. of the shafts are given in Tables 4 and 5 for 1.5 ft. thickness, which is estimated to be adequate. The checking of stresses and ductility is presented in the following :

#### (a) Elastic Design

The maximum combined moment due to eccentricity of load and earthquake force occurs at R. L. 1407.5 ft. At this section the vertical load is as follows :

$$P = 380 + \pi \times 13.5 \times 1.5 \times 0.150 \times 22.5 = 595 \text{ kips}$$

$$\text{Maximum moment} \quad M = 8663 \text{ kip. ft.}, \quad (\text{see Table 4})$$

$$\text{Maximum Shear Force} \quad F = 205.9 \text{ kips}$$

Let the shaft be uniformly reinforced with 0.7% steel of the concrete cross section. Hence thickness of steel ring,  $t_s = 0.007t$  where  $t$  = thickness of shaft, that is, 18 in.

Balancing the moments of the effective areas about the N.A. (see Fig. 8), we get

$$\int_0^a [t + (m-1)t_s] r^2 (\cos \theta - \cos a) d\theta = \int_0^{\pi-a} m t_s r^2 (\cos \theta + \cos a) d\theta$$

$$\text{or, } (t - t_s) (\sin a - a \cos a) - m t_s \pi \cos a = 0$$

Substituting the values of  $t$  and  $t_s$ , and  $m=13$

$$0.093 (\sin a - a \cos a) - 0.286 \cos a = 0$$

Table 4

## Distribution of Moments Along Height\*

Section (1)	Moments in kip ft due to				
	Ecc. of shaft House (2)	El Centro peak 0.17g (3)	Combined (4)=(2)+(3) (4)	El Centro Peak 0.33g (5)	Combined (6)=(2)+(3) (6)
Shaft house 1457.5	0.0	0.0	0.0	0.0	0.0
1447.0	0.0	622	622	1210	1210
1430.0	2660	3105	5765	6038	8698
1425.5	2660	4010	6670	7787	10447
1421.0	2623	4900	7523	9503	12126
1416.5	2532	5640	8172	10956	13488
1412.0	2283	6180	8563	12008	14391
1407.5	2183	6480	8663	12591	14774
1403.0	1946	6535	8481	12698	14644
Shaft 1398.5	1688	6360	8048	12367	14055
1394.0	1428	6000	7428	11663	13091
1389.5	1174	5490	6664	10669	11843
1385.0	936	4876	5812	9473	10409
1380.5	718	4200	4918	8158	8876
1376.0	523	3500	4023	6796	7319
1371.5	355	2800	3155	5444	5799
1367.0	210	2130	2340	4144	4354

\* Larger of the values for shafts  $T_1$  and  $T_2$ .

Table 5  
Distribution of Shears\*

Section (1)	Shear in kips due to				
	Ecc. of shaft house (2)	El Centro peak 0.17g (3)	Combined (4)=(3)+(2)	El Centro Peak 0.33g (5)	Combined (6)=(2)+(5)
1457.5	0.0	57.0	57.0	110.9	110.9
1447.0	0.0	144.0	144.0	279.6	279.0
1430.0	8.2	197.7	205.9	384.4	392.6
1425.5	20.3	194.0	214.3	377.0	397.3
1421.0	33.1	164.2	197.3	319.2	352.3
1416.5	44.4	118.5	162.9	230.1	274.5
1412.0	52.7	65.2	117.9	126.4	179.1
1407.5	57.3	10.8	68.1	21.0	78.3
1403.0	57.8	39.1	96.9	76.1	133.9
1398.5	56.3	81.5	137.8	158.5	214.8
1394.0	53.0	114.5	167.5	222.5	275.5
1389.5	48.5	137.5	186.0	267.1	315.6
1385.0	43.1	151.0	194.1	293.3	336.4
1380.5	37.5	156.0	193.5	303.5	341.0
1376.0	32.0	155.0	187.0	300.9	342.9
1371.5	27.0	149.0	176.0	289.4	316.4
1367.0	22.8	134.5	157.3	261.0	283.8
1362.5	19.4	118.5	137.9	229.6	239.0
1358.0					

\* Values are given irrespective of sign.

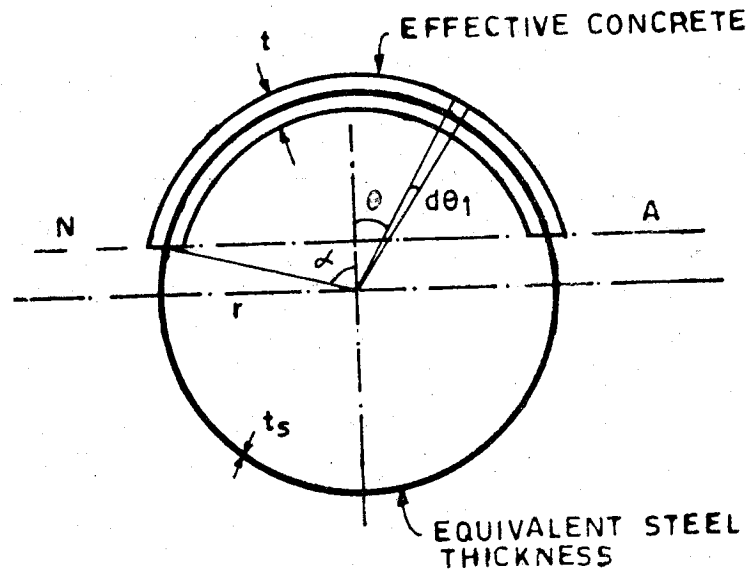


Fig. 8. Elastic Analysis of Section

Solving by trials,  $\alpha = 0.85$  radian.

Now moment of inertia of effective section about N. A.,

$$I = 2 \int_0^{\alpha} [t + (m-1)t_s] r^3 (\cos \theta - \cos \alpha)^2 d\theta + 2 \int_0^{\pi-\alpha} m t_s r^3 (\cos \theta + \cos \alpha)^2 d\theta$$

or

$$I = 2 r^3 \left\{ [t + (m-1)t_s] \left[ \frac{1}{2} \alpha^2 + \cos^2 \alpha \right] - \frac{3}{4} \sin 2\alpha \right\} + m t_s \left\{ (\pi - \alpha) \left[ \frac{1}{2} + \cos^2 \alpha \right] + \frac{3}{4} \sin 2\alpha \right\}$$

$$= \pi r^3 m t_s (1 + 2 \cos^2 \alpha) + r^3 (t - t_s) \{ (1 + 2 \cos^2 \alpha) - 3 \sin \alpha \cos \alpha \}$$

Substituting the various values,

$$I = 6.07 \times 10^6 \text{ in}^4$$

$$\text{Area of section A} = 0.007 \times 18 \times 2\pi \times 6.75 \times 12 + 18 \times 2 \times 0.85 \times 6.75 \times 12$$

$$= 835 + 2480 = 3315 \text{ in}^2$$

$$\text{Tensile stress in steel} = 13 \left[ -\frac{595000}{3315} + \frac{8663000 \times 12}{6.07 \times 10^6} \times 6.75 (1 + 0.66) \times 12 \right]$$

$$= 27570 \text{ psi}$$

This is less than the yield stress  $\sigma_{sy}$  of steel 34000 psi, and hence is safe. Compressive stress in concrete

$$= \frac{595000}{3315} + \frac{8663000 \times 12}{6.07 \times 10^6} = 3.04 \times 12$$

$$= 805 \text{ psi (safe)}$$

Therefore 18 inches thickness with 0.7% vertical steel is adequate. Now the static moment of the area of the section lying above the natural axis taken about the neutral axis is,

$$\begin{aligned} A\bar{y} &= 2m t_s [\sin \alpha + (\pi - \alpha) \cos \alpha] r^2 \\ &= 4.82 \times 10^4 \text{ in}^3 \end{aligned} \quad (11)$$

$$\begin{aligned} \text{Max. shear stress} &= \frac{205900 \times 4.82 \times 10^4}{6.07 \times 10^6 \times 18 \times 2} \\ &= 45.5 \text{ psi (safe)} \end{aligned}$$

The hoop steel may be kept a minimum of 0.3% of the concrete section except where it is required to be more due to other loads such as hydrostatic pressure inside.

(b) *Plastic Design*

The plastic moment capacity  $M_p$  of the section of shaft may be worked out on the basis of yielding of steel alone, the concrete being neglected.

$$M_p = \sigma_{sy} Z_p = \sigma_{sy} f Z \quad (12)$$

where  $Z_p$  is the plastic modulus of section,  $f$  the shape factor equal to 1.27 for thin circular section and  $Z$  the elastic modulus of section. Therefore

$$M_p = 34.0 \times 1.27 (\pi \times 6.75^2 \times 144 \times 0.007 \times 18) / 12 = 9380 \text{ kip-ft.}$$

A reasonable estimate of the ductility ratio attained, when the El Centro (Peak acc. 0.33 g) earthquake acts, may be obtained by equating the elastic strain energy with the plastic energy as shown in Fig. 9 in the following manner.

If the structure would have remained elastic, and the moment was  $M_e$  (which in this case is 1477 kip ft. as given in Table 4 (b)) and curvature  $\theta_e$ , then the elastic strain energy would have been

$$\begin{aligned} U_e &= \frac{1}{2} M_e \theta_e \\ &= \frac{1}{2} \frac{M_e^2}{M_p} \theta_y \end{aligned} \quad (13)$$

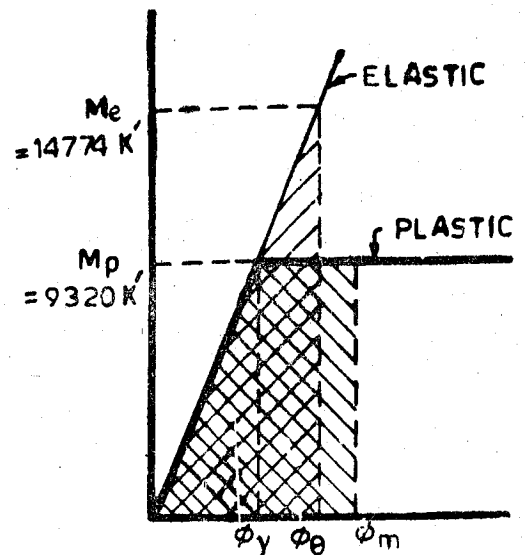


Fig. 9. Energy Equivalence

where  $\theta_y$  is the curvature corresponding to the start of plasticity, shown in Fig 8. Now if the structure actually deforms plastically to maximum curvature  $\theta_m$ , the energy absorbed would be

$$U_p = M_p (\theta_m - \frac{1}{2} \theta_y)$$

Equating  $U_e$  to  $U_p$ , we get

$$\theta_m - \frac{1}{2} \theta_y = \frac{1}{2} \left( \frac{M_e}{M_p} \right)^2 \theta_y$$

Or the ductility ratio  $\theta_m/\theta_y$  is given by

$$\frac{\theta_m}{\theta_y} = \frac{1}{2} \left[ \left( \frac{M_e}{M_p} \right)^2 + 1 \right] \quad (15)$$

Substituting the value of  $M_e$  and  $M_p$ ,

$$\frac{\theta_m}{\theta_y} = \frac{1}{2} \left[ \left( \frac{14764}{9320} \right)^2 + 1 \right] = 1.755$$

This is much less than 4, hence the shaft will be safe in the maximum earthquake expected at site.

### CONCLUSIONS

The following general conclusions may be drawn from the results presented in this paper.

- (1) The soil offers substantial resistance against the deflections of the shaft increasing the effective stiffness and consequently the frequency.
- (2) In the behaviour of the buried shafts, their critical length  $L_c$  turns out to a very important parameter as their bending mostly takes place in this length below the ground level. Consequently, where  $L_c$  is smaller than the actual length of a shaft, the maximum moments caused in a shaft in soil will be much smaller than the shaft in air. The reduction in the cases presented is about 70%. Also the point of maximum moment will shift towards the top near about the point at  $L_c$  below ground level.
- (3) Damping to the vibrations is increased because of the presence of soil around the shafts, 10% of critical will be a conservative value for adopting for design purposes.
- (4) The indications are that no virtual soil mass acts in the dry condition. However, this point needs further testing to arrive at final conclusion.
- (5) The ordinary static seismic coefficient method is rather inadequate for aseismic design of such tall structures. Therefore dynamic analysis is strongly recommended.

### ACKNOWLEDGEMENT

The authors are grateful to Dr. Jai Krishna, Director, School of Research and Training in Earthquake Engineering, University of Roorkee, Roorkee for his constant encouragement throughout these investigations. The grant for this project was provided by the Beas Project, Talwara Township, Punjab.

### REFERENCES

1. Abbet, R.W., "American Civil Engineering Practice", Vol. III, Section 34, John Wiley and Sons, Inc., New York, 1957.
2. Davisson, M.T., "Estimating Buckling Loads for Piles", Proc. of II Panamerican Conference of Soil Mech. and Foundation Engineering, Vol. I, July 1963.
3. Housner, G.W., P.R. Martel, and J.L. Alford, "Spectrum Analysis of Strong Motion Earthquakes", Bull. S S A Vol. 43, No. 2, April 1953.
4. IS : 1893—1966, Criteria for Earthquake Resistant Design of Structures (Cl. 6.4.2, p. 21).
5. Matlock, H. and L.C. Reese, "Generalised Solutions, A. S. C. E., Paper No. 3370, Vol. 127, 1962, Part I pp. 1220-1251.
6. Tarzagli, Karl, "Evaluation of Coefficients of Subgrade Reaction", Geotechnique, Vol. 5, pp. 297, 1955.